AGU PUBLICATIONS

Geophysical Research Letters

Supporting Information for

Type-dependent responses of ice cloud properties to aerosols from satellite retrievals

Bin Zhao[1, 2], Yu Gu[1], Kuo-Nan Liou[1], Yuan Wang[2, 3], Xiaohong Liu[4], Lei Huang[1, 2], Jonathan H. Jiang[2], and Hui Su[2]

[1]Joint Institute for Regional Earth System Science and Engineering and Department of Atmospheric and Oceanic Sciences, University of California, Los Angeles, California 90095, USA.

[2]Jet propulsion Laboratory, California Institute of Technology, Pasadena, California 91109, USA.

[3]Division of Geological and Planetary Sciences, California Institute of Technology, Pasadena, California 91109, USA.

[4]Department of Atmospheric Science, University of Wyoming, Laramie, Wyoming 82071, USA.

Corresponding authors: Bin Zhao (zhaob1206@ucla.edu) and Yu Gu (gu@atmos.ucla.edu)

Contents of this file

Introduction

This document includes supplementary methods, figures and tables, which have been cited in the main text.

Text S1. Impact of ICF calculation method

As described in Section 2.1 in the main text, we only include in ICF calculation the MODIS ice pixels within a 20 km radius that vertically overlap with the CALIOP ice cloud layer (Layer Top Pressure of CALIOP ice cloud layer – 10 hPa ≤ Cloud Top Pressure of MODIS ice pixel ≤ Layer Base Pressure of CALIOP ice cloud layer), in order to minimize contamination by the cloud pixels that does not belong to the same cloud layer as detected by CALIOP. Here 10 hPa corresponds to about 0.25 km at the ice cloud altitude. The ICF calculated using this baseline method is denoted by "ICF" in Fig. S1. We have conducted a sensitivity test in which all valid ice cloud pixels within the 20 km radius are accounted for, whether or not they vertically overlap with the CALIOP ice cloud layer (denoted by "ICF_overlap+nonoverlap" in Fig. S1). The ICF calculated using the sensitivity method ("ICF_overlap+nonoverlap") is 0.05 to 0.07 higher than the baseline ("ICF"). Nevertheless, the relationships between ICF and AOD are very similar under these two calculation methods.

Moreover, we performed two sensitivity tests in which ICF is calculated following the baseline method ("ICF" in Fig. S1), except that 10 km and 5 km radii are used (denoted by "ICF_10km" and "ICF_5km" in Fig. S1) instead of a 20 km radius. The usage of smaller radii further increases the likelihood that MODIS ice pixels included in ICF calculations belong to the same cloud as detected by CALIOP. Fig. S1 illustrates that the magnitude of ICF increases remarkably as the radius for calculations is reduced. However, the relationship pattern between ICF and AOD remains unchanged. In this study, we have retained a 20 km radius in order to investigate the aerosol impact on cloud horizontal development over a relatively large spatial scale.

In the present study, partly cloudy ice pixels in MODIS are excluded from the ICF calculations following the method to calculate ICF in MODIS Level 3 product [*Hubanks et al.*, 2016], because the retrievals for partly cloudy pixels are subject to large uncertainties [*Platnick et al.*, 2015a]. To examine the impact of partly cloudy pixels on the ICF calculations, we performed a sensitivity test in which partly cloudy pixels (i.e., those with "clear sky restoral flag" of 1 or 3 [*Platnick et al.*, 2015a]) are included, assuming that one partly cloudy pixel accounts for 0.5 overcast pixel ("ICF_pcl" in Fig. S1). The magnitude of ICF calculated with partly cloudy pixels is 0.01-0.04 larger than that without partly cloudy pixels, but the responses of ICF to aerosols are similar in these two cases.

Text S2. Discussions about the IWP and IWC retrievals

In this study, the IWP and IWC retrievals are obtained from a CloudSat-CALIOP combined product (2C-ICE, version P1_R04), which is reported in the same resolution (1.7 km along-track and 240 m vertically) as other CloudSat retrieval products. To collocate the 2C-ICE product with the CALIOP 05kmMLay product at a 5 km along-track resolution, we horizontally average the 2C-ICE IWC and IWP retrievals at 1.7 km resolution within the range of a CALIOP 5 km profile. In the vertical direction, the 2C-ICE IWC data are vertically averaged between the top and bottom of the ice cloud layer retrieved by CALIOP. The average thickness of ice cloud layers is about 1.3 km, corresponding to 5-6 2C-ICE vertical bins.

The algorithm used to generate the 2C-ICE product enables the retrieval of ice cloud properties in three cloud regions: (1) a lidar-only region consisting of high tenuous clouds detected only by CALIOP, (2) a radar/lidar overlapped region where CloudSat and CALIOP both sense the presence of cloud, and (3) a radar-only region in which CALIOP signal has been fully attenuated but CloudSat continues to return data [*Mace and Deng*, 2015]. This study focuses on single-layer ice-only clouds, which are primarily optically thin cirrus clouds that seldom fully attenuate the CALIOP lidar signal. For this reason, among the samples used in our analysis, 65%, 33%, and 2% are located in the lidar-only, radar-lidar overlapped, and radar-only regions, respectively. As the 2C-ICE and CALIOP products both incorporate lidar measurements, their sensitivities to ice crystal size should be similar. For this reason, it appears reasonable to collocate the 2C-ICE and CALIOP products.

We did not use IWP from CALIOP because the CALIOP IWC (and hence IWP) retrieval is a provisional data product. "Provisional" means that only limited comparisons with independent sources have been made and artifacts have not been fully fixed, thus more validation is still needed. Also, CALIOP IWC is calculated as a simple parameterized function of the CALIOP-retrieved extinction coefficients [*NASA CALIPSO team*, 2012a]:

$$\mathrm{IWC} = C_0\left(\frac{\sigma}{1000}\right)^{C_1}$$

where σ is the 532 nm volume extinction coefficient in km^{-1}, and $C_0 = 119$ g m^{-3} and $C_1 = 1.22$ are coefficients derived from an observed empirical relationship between lidar extinction and in situ measurements of cloud particle properties. For this reason, the IWP-aerosol relationships will obviously be very similar to the COT-aerosol relationships, therefore it makes little sense to include CALIOP IWC/IWP.

In contrast, the usage of IWC/IWP from the 2C-ICE CloudSat-CALIOP combined retrieval product could serve as an independent support for the relationships between COT and aerosols found in this study. We believe that the IWC retrieval from the 2C-ICE product is better than that from the CALIOP product because of two reasons. First, 33% of the samples used in our analysis are located in the radar-lidar overlapped regions, in which the IWC retrievals from 2C-ICE incorporate both lidar and radar measurements. Second, even in the lidar-only region, the 2C-ICE product makes use of a more sophisticated retrieval algorithm based on an optimal estimation framework [*Mace and Deng*, 2015]. In this framework, the relationships between the vertical profiles of the ice cloud microphysical properties (IWC, effective radius, etc.) and lidar attenuated backscattering coefficients are developed and a look-up table is subsequently built. Then, the ice cloud microphysical properties are optimized based on the measured attenuated backscattering coefficients.

Text S3. Evaluating the effects of meteorological covariation

We have examined the responses of column AOD to ten meteorological parameters that may significantly affect the formation and evolution of ice clouds (as listed in Table S3) in our previous study [*Zhao et al.*, 2018], and found that AOD does not show large changes in response to variation in any of the ten meteorological parameters (see Fig. S3 in [*Zhao et al.*, 2018]). Here we have repeated this analysis for layered AOD in case of in-situ formed ice clouds, and the results are illustrated in Fig. S3. Similar to the results for column AOD, we find that layer AOD does not have large changes in response to variation in any meteorological parameter. Particularly, there are indeed some positive correlations between layer AOD and relative humidity averaged between 100 hPa and 440 hPa ($RH_{100\text{-}440hPa}$). However, layer AOD only increases by about 10% from the smallest to the largest $RH_{100\text{-}440hPa}$ bin. The magnitude of change is significantly smaller than the relationships between COT (or ICF, cloud thickness) and layer AOD in case of in-situ formed ice clouds (Fig. 1d in main text).

Besides, we have calculated the partial correlation between AOD and ice cloud properties following the method used in *Engstrom and Ekman* [2010], in order to exclude the impact of meteorological covariation at reanalysis data resolution. The partial correlation is a measure of the linear dependence between two variables where the influence from possible controlling variables (meteorological parameters in this case) is removed [*Engstrom and Ekman*, 2010; *Hardle and Simar*, 2015; *Johnson and Wichern*, 2007; *PSU*, 2017]. Let X denote a vector of meteorological parameters, the effects of which we would like to eliminate. The partial correlation between AOD and COT (or ICF, cloud thickness), eliminating the effects of X, is:

$$\rho_{AOD-COT.X} = \frac{\sigma_{AOD-COT.X}}{\sigma_{AOD.X}\sigma_{COT.X}}$$

where $\sigma_{AOD-COT.X}$ is the conditional covariance between AOD and COT, eliminating the effects of X; $\sigma_{AOD.X}$ is the square root of the conditional variance of AOD, eliminating the effects of X; $\sigma_{COT.X}$ is the square root of the conditional variance of COT, eliminating the effects of X. More details of the calculation method for partial correlation are described in several mathematical textbooks [*Hardle and Simar*, 2015; *Johnson and Wichern*, 2007; *PSU*, 2017].

Here we calculate the partial correlations with the effects of 10 meteorological parameters (listed in Table S3) removed simultaneously, and compare with the total correlations. We also perform two additional groups of calculations in which only the effects of $RH_{100\text{-}440hPa}$ and the vertical velocity at 300 hPa (VV300) are eliminated, respectively. The results are summarized in Table S4. Note that we computed the total and partial correlations between column AOD and ice cloud properties for all ice cloud types, as well as those between layer AOD and ice cloud properties for in-situ formed ice clouds. We do not perform partial relation calculations for convection-generated ice clouds since the responses of ice cloud properties to AOD are not monotonic in this case.

For all cases, the total and partial correlations are generally similar. In the cases where the partial correlation is smaller than the total correlation, which means that meteorological covariation could partly explain the aerosol-cloud relationship, the difference between the partial and total correlations are all within 24%. In particular, the partial correlations between layer AOD and ICF/cloud thickness/COT of in-situ ice clouds with the effect of $RH_{100\text{-}440hPa}$ eliminated are 21%/2%/0% smaller than the corresponding total correlations. Therefore, the comparison between total and partial relations indicates that the meteorological covariations at reanalysis data resolution does not appear to be major causes for the relationships between aerosols and ice cloud properties, though they can indeed play some minor roles in certain situations.

Note that reanalysis data may not be sufficiently representative of the real atmosphere to completely remove the effects of meteorological covariation on the aerosol-cloud relationships [*Gryspeerdt et al.*, 2016]. In particular, the relative humidity shows a strong small- to mesoscale variability that could be important for the aerosol swelling and cloud formation and cannot be constrained by reanalysis products with resolutions of tens of kilometers [*Gryspeerdt et al.*, 2016]. The quantitative assessment of the meteorological covariation at smaller scales is a very complicated and difficult task that merits further in-depth study.

Text S4. Effect of contaminations in AOD and cloud retrievals

A cloud contamination in AOD retrievals [*Kaufman et al.*, 2005] could cause an artificial positive correlation between AOD and ice cloud properties. Such contamination is more likely to occur for high AOD retrievals. Nevertheless, strong positive correlations between AOD and cloud thickness/COT/ICF mainly occur at small AOD range, while the correlations are quite weak (even slightly negative) at higher AOD range (Fig. 1a).

Also, we conducted a sensitivity analysis following *Koren et al.* [2010]. In the sensitivity case, AOD is calculated using 10 km×10 km AOD retrievals that report less than 20% cloud fraction within the 10 km×10 km area. *Koren et al.* [2010] suggested that the 20% cloud fraction cut-off corresponds to an average distance of 5 km between a pixel used by the AOD retrieval and an identified cloudy pixel. There is no guarantee that this procedure eliminates all possible cloud contamination, but most of the pixels likely to be cloud contaminated are filtered out [*Koren et al.*, 2010]. Figure. S4 illustrates the changes in ICF, cloud thickness, and COT with aerosols in the base and sensitivity cases. The responses of all three cloud properties to AOD are very similar under the base and sensitivity cases, although the magnitude of changes is slightly smaller in the sensitivity case. For this reason, the contamination of AOD retrievals by clouds does not seem to be a major cause for the aerosol-cloud relationships.

Text S5. Impact of retrieval uncertainties

The CALIPSO team has performed a detailed assessment of uncertainties in individual COT retrievals [*NASA CALIPSO team*, 2010], which has been incorporated in the 05kmMLay product used in this study. The assessment assumed that all uncertainties were random and uncorrelated. Although this is not always strictly true, it was considered adequate for estimating the influences of main uncertainties [*NASA CALIPSO team*, 2010]. Following this assumption, we use the propagation of uncertainty formula to estimate the retrieval uncertainty in average COT within each AOD bin in Figs. 1 and 2. The results show that the COT retrieval uncertainties are less than 0.003 for all AOD bins in Fig. 1a that illustrates overall changes in COT with reference to AOD. The uncertainties are less than 0.012 in all other figures that show COT changes for individual ice cloud types and/or meteorological ranges. The magnitude of retrieval uncertainty is significantly smaller than the COT trends in response to AOD. While we have considered all error sources as random uncertainties following *NASA CALIPSO team* [2010], it should be noted that some of them might be systematic errors. For example, a systematic overestimation in lidar ratio adopted in the retrieval algorithm could subsequently lead to an overestimation in retrieved COT. However, the possible systematic retrieval errors have not yet been quantified by any previous study.

For ICF and the cloud thickness, the retrieval products used in this study do not provide uncertainty assessment. It is very difficult to quantitatively evaluate retrieval uncertainties. The ICF is calculated using the ratio of the number of MODIS ice-phase pixels to the number of all pixels within a 20 km radius of a CALIOP profile. The ICF uncertainty would depend on the reliability in determining the existence and phase of clouds in individual MODIS pixels. We only included in the ICF calculation the pixels whose "primary cloud retrieval outcome" is successful, which would reduce uncertainty in cloudy pixel identification. Furthermore, we have tested a number of ICF calculation methods involving different thresholds for selecting ice pixels, as detailed in Text S1. These results indicate that the responses of ICF to aerosols are similar for all calculation methods, implying that these responses are unlikely explained by retrieval errors or calculation methods. Similar to ICF, the uncertainty in cloud thickness retrieval depends on the confidence in the determination of cloud existence, especially near cloud top and bottom where the cloud becomes relatively thin. If we assume that two 30 m vertical bins are randomly misclassified at the top and bottom of a cloud, the retrieval uncertainties of average cloud thickness within AOD bins used in Figs. 1-2 are estimated to be less than 4 m, much smaller than the magnitude of cloud thickness trends in response to aerosols.

For AOD, comparison studies with AERONET have estimated the accuracy of MODIS AOD retrievals to be about $\pm 0.05 \pm 0.15 \times$ AOD over land and $\pm 0.03 \pm 0.05 \times$ AOD over ocean [*Levy et al.*, 2010; *Remer et al.*, 2005]. This error magnitude could result in some samples being put into a neighboring AOD bin in Figs. 1 and 2, but should not noticeably affect the overall responses of ice cloud properties to AOD changes from the smallest to the largest bins.

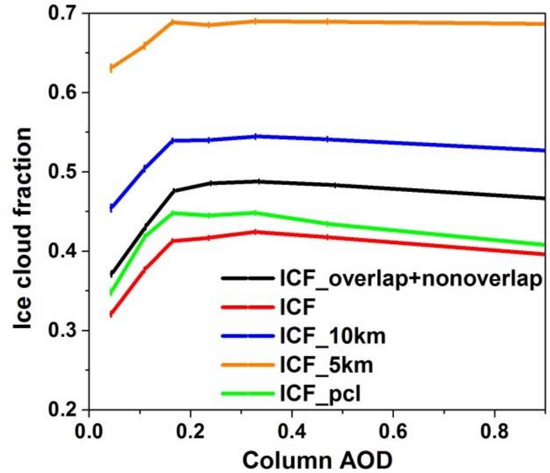

Figure S1. Responses of ICF of all ice cloud types calculated using different methods to AOD changes.

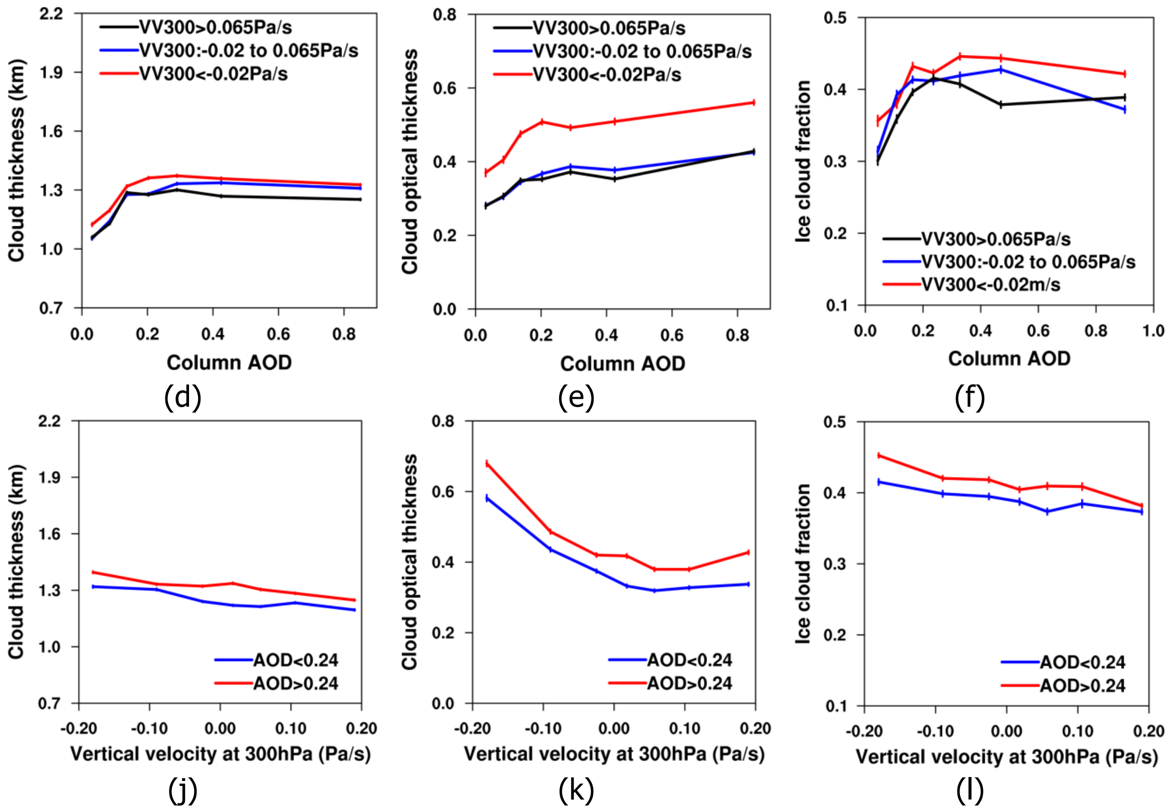

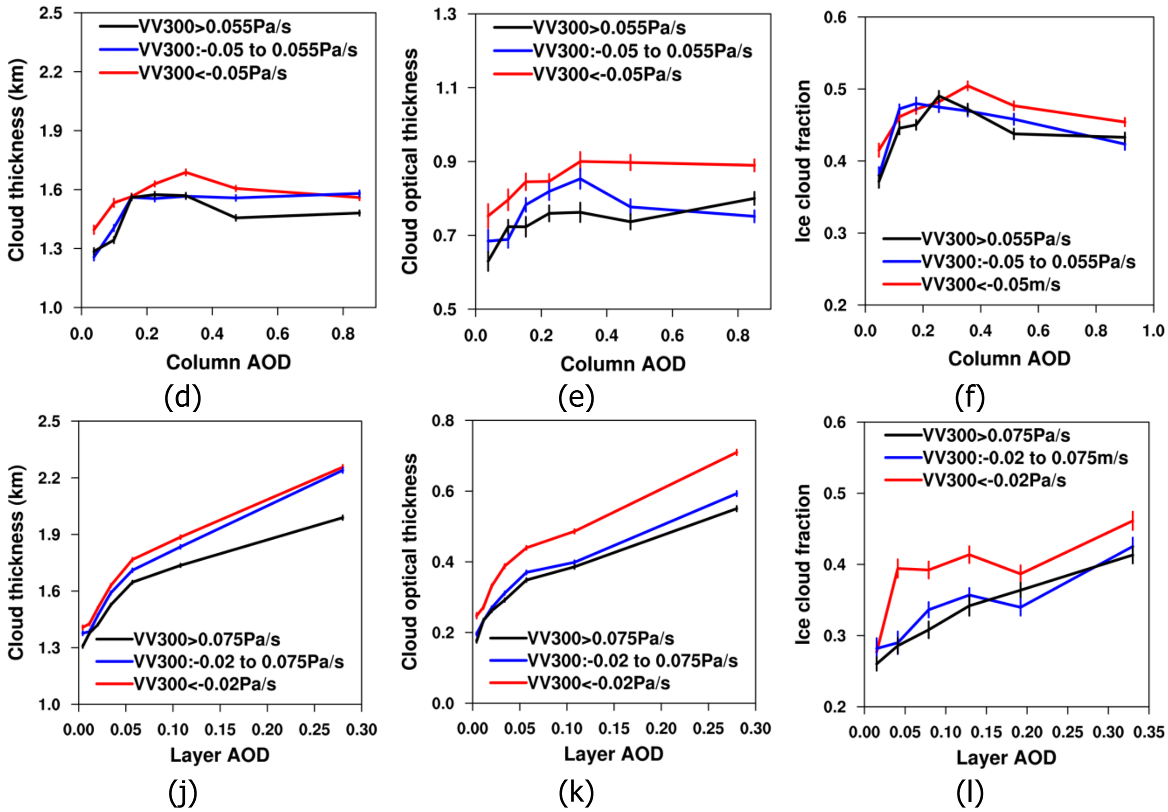

Figure S2. The same as Fig. 2 in the main text but for pressure vertical velocity at 300 hPa (VV300). Negative VV300 values indicate net upward air motion, whereas positive VV300 values indicate net subsidence.

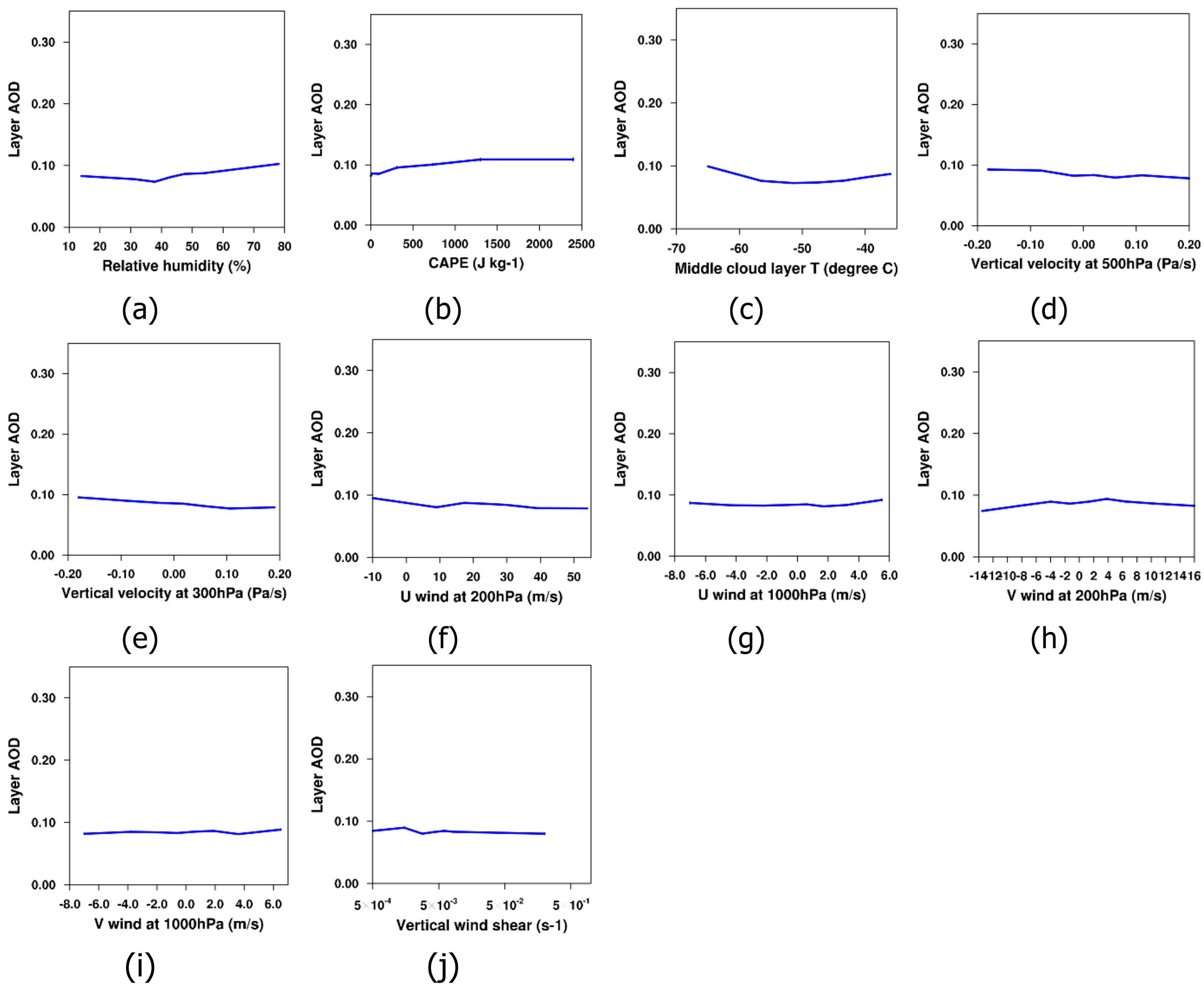

Figure S3. Changes in layer AOD mixed with in-situ formed iced clouds as a function of meteorological parameters: (a) $RH_{100\text{-}440hPa}$, (b) convective available potential energy, (c) middle cloud layer temperature, (d) vertical velocity at 500 hPa (VV500), (e) VV300, (f) U-components of wind speed at 200 hPa, (g) U-components of wind speed at 1000 hPa, (h) V-components of wind speed at 200 hPa, (i) V-components of wind speed at 1000 hPa, (j) and vertical wind shear at potential vorticity surface of 2×10^{-6} deg K m^2 kg^{-1} s^{-1}. The error bars represent the standard errors ($\sigma/\sqrt{N}$), in which σ is the standard deviation and N is the number of samples. The error bars in some panels are very small and therefore invisible.

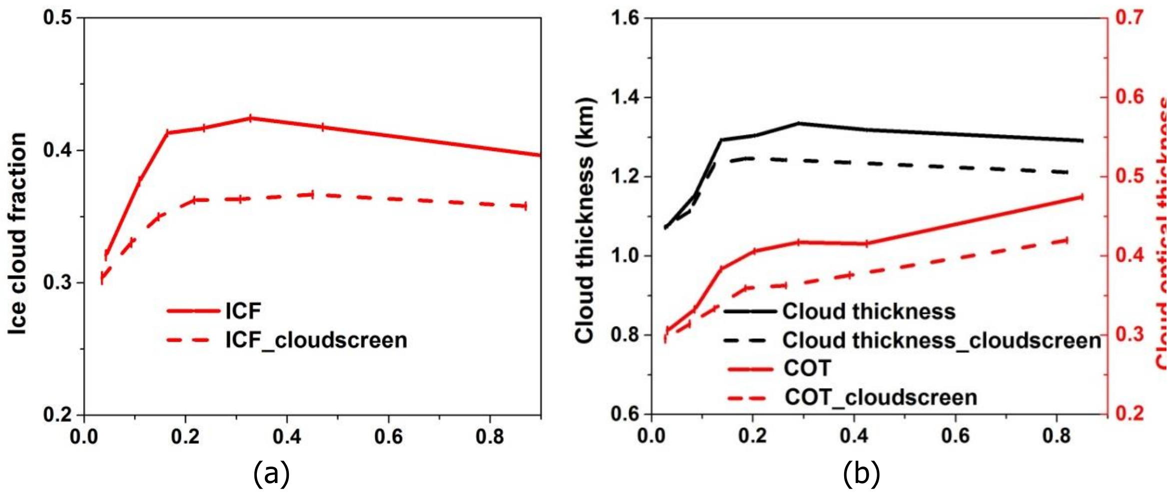

Figure S4. Changes in (a) ICF and (b) cloud thickness and COT with aerosols in the base case and a sensitivity case (denoted by a suffix of "cloudscreen") in which AOD retrievals with high cloud fraction (>20%) are filtered.

Table S1. Datasets used in this study.

Satellite/ Sensor	Product	Variable	Horizontal resolution
Aqua/MODIS	MYD04 (Level 2, Collection 6) [*Levy et al.*, 2015]	Column AOD	10 km × 10 km
	MYD06 (Level 2, Collection 6) [*Platnick et al.*, 2015b]	Primary cloud retrieval outcome and cloud phase (determined by the "cloud optical property" algorithm)	1 km × 1 km
CALIPSO/ CALIOP	05kmMLay (Level 2, V4.10) [*NASA CALIPSO team*, 2012b]	Aerosol/cloud layer number, layer aerosol/cloud optical depth, layer top/base height (cloud thickness is derived from the difference between the two), layer base temperature, middle layer temperature, feature classification flags (containing the "aerosol type" and "cloud type" flags), extinction QC, and CAD score	5 km along-track
	05kmAPro (Level 2, V4.10) [*NASA CALIPSO team*, 2012a]	Vertically resolved relative humidity*	5 km along-track
CloudSat/CPR	2C-ICE (Level 2, Version P1_R04) [*Mace and Deng*, 2015]	Ice water path, vertically resolved ice water content	1.7 km along-track
--	NCEP ds083.2 [*National Centers for Environmental Prediction/National Weather Service/NOAA/U.S. Department of Commerce*, 2000]	Vertically resolved wind speed & pressure vertical velocity; wind shear; convective available potential energy	1º × 1º

* The relative humidity in the 05kmAPro product was adapted from the GEOS-5 data product provided to the CALIPSO project by the GMAO Data Assimilation System.

Table S2. Changes in ice cloud properties from the lowest third to the highest third AOD subsets.

Cloud type	Cloud property	Mean of the lowest subset	Mean of the highest subset	Absolute change	Fractional change
All types	Cloud thickness	1.174	1.305	0.131	11.2%
	COT	0.341	0.445	0.104	30.7%
	ICF	0.426	0.475	0.049	11.5%
Convective	Cloud thickness	1.429	1.543	0.114	8.0%
	COT	0.732	0.813	0.080	10.9%
	ICF	0.508	0.533	0.025	5.0%
In-situ	Cloud thickness	1.409	1.996	0.587	41.6%
	COT	0.247	0.525	0.278	112.8%
	ICF	0.335	0.457	0.122	36.5%

Note: considering the different criteria for the selection of valid data points for all, convective, and in-situ ice cloud types (the former two requires valid column AOD from MODIS and the last type requires valid layer AOD from CALIOP), the weighted-average cloud properties of convective and in-situ ice clouds may not equal the properties of all ice cloud types.

Table S3. Correlation coefficients between major ice cloud properties and the meteorological variables that can affect the development of ice clouds.

	Cloud thickness	COT	ICF
Relative humidity averaged between 100 hPa and 440 hPa	**0.196**	-0.016	**0.153**
Middle cloud layer temperature	0.032	**0.249**	**-0.065**
Convective available potential energy	**0.083**	0.034	**0.145**
Pressure vertical velocity at 500 hPa	-0.017	**-0.066**	**-0.072**
Pressure vertical velocity at 300 hPa	**-0.054**	**-0.080**	**-0.104**
U-component of wind speed at 200 hPa	**-0.092**	0.033	**-0.086**
U-component of wind speed at 1000 hPa	-0.013	0.029	-0.050
V-component of wind speed at 200 hPa	-0.027	0.020	0.050
V-component of wind speed at 1000 hPa	0.034	0.023	*-0.003*
Vertical wind shear	-0.022	*0.004*	0.015

Note: The numbers in bold indicate correlations coefficients greater than ±5%; the italic numbers are not statistically significant at the 0.01 level based on the Student's t-test.

Table S4. Total correlations between column/layer AOD and ice cloud properties and the corresponding partial correlations with the effects of certain meteorological parameters eliminated. The numbers in brackets are 95% confidence intervals.

Cloud properties	Total correlation	p-value	Partial correlation eliminating effects of 10 parameters	p-value	Partial correlation eliminating effect of $RH_{100\text{-}440hPa}$	p-value	Partial correlation eliminating the effects of VV300	p-value
Column AOD vs. all ice cloud types								
ICF	0.031 (0.023, 0.040)	< 0.001	0.043 (0.034, 0.052)	< 0.001	0.040 (0.032, 0.049)	< 0.001	0.031 (0.022, 0.039)	< 0.001
Cloud thickness	0.031 (0.027, 0.035)	< 0.001	0.043 (0.039, 0.047)	< 0.001	0.042 (0.039, 0.046)	< 0.001	0.030 (0.026, 0.034)	< 0.001
COT	0.097 (0.094, 0.102)	< 0.001	0.085 (0.081, 0.090)	< 0.001	0.097 (0.093, 0.101)	< 0.001	0.095 (0.092, 0.100)	< 0.001
Layer AOD vs. in-situ formed ice clouds								
ICF	0.168 (0.150, 0.195)	< 0.001	0.128 (0.109, 0.153)	< 0.001	0.132 (0.113, 0.157)	< 0.001	0.166 (0.148, 0.193)	< 0.001
Cloud thickness	0.252 (0.249, 0.261)	< 0.001	0.245 (0.241, 0.253)	< 0.001	0.246 (0.242, 0.254)	< 0.001	0.251 (0.247, 0.259)	< 0.001
COT	0.204 (0.200, 0.211)	< 0.001	0.193 (0.189, 0.200)	< 0.001	0.204 (0.200, 0.210)	< 0.001	0.202 (0.198, 0.209)	< 0.001

References

Engstrom, A., and A. M. L. Ekman (2010), Impact of meteorological factors on the correlation between aerosol optical depth and cloud fraction, *Geophys Res Lett*, *37*.

Gryspeerdt, E., J. Quaas, and N. Bellouin (2016), Constraining the aerosol influence on cloud fraction, *J Geophys Res-Atmos*, *121*(7), 3566-3583.

Hardle, W. K., and L. Simar (2015), *Applied Multivariate Statistical Analysis, fourth edition*, Springer, Berlin, Germany.

Hubanks, P., S. Platnick, M. King, and B. Ridgway (2016), MODIS Atmosphere L3 Gridded Product Algorithm Theoretical Basis Document (ATBD) & Users Guide.

Johnson, R. A., and D. W. Wichern (2007), *Applied Multivariate Statistical Analysis, sixth edition*, Pearson Education Inc., New Jersey, U.S.A.

Kaufman, Y. J., I. Koren, L. A. Remer, D. Rosenfeld, and Y. Rudich (2005), The effect of smoke, dust, and pollution aerosol on shallow cloud development over the Atlantic Ocean, *P Natl Acad Sci USA*, *102*(32), 11207-11212.

Koren, I., G. Feingold, and L. A. Remer (2010), The invigoration of deep convective clouds over the Atlantic: aerosol effect, meteorology or retrieval artifact?, *Atmos Chem Phys*, *10*, 8855–8872.

Levy, R. C., C. Hsu, A. Sayer, S. Mattoo, and J. Lee (2015), MODIS Atmosphere L2 Aerosol Product. doi:10.5067/MODIS/MYD04_L2.006, NASA MODIS Adaptive Processing System, Goddard Space Flight Center.

Levy, R. C., L. A. Remer, R. G. Kleidman, S. Mattoo, C. Ichoku, R. Kahn, and T. F. Eck (2010), Global evaluation of the Collection 5 MODIS dark-target aerosol products over land, *Atmos Chem Phys*, *10*(21), 10399-10420.

Mace, G. G., and M. Deng (2015), Level 2C CloudSat-CALIPSO Combined Ice Cloud Property Retrieval Product Process Description Document, available at http://www.cloudsat.cira.colostate.edu/sites/default/files/products/files/2C-ICE_PDICD.P1_R04.20151104.pdf.

NASA CALIPSO team (2010), Uncertainty Analysis for Particulate Backscatter, Extinction and Optical Depth Retrievals reported in the CALIPSO Level 2, Version 3 Data Release.

NASA CALIPSO team (2012a), CALIPSO Quality Statements: Lidar Level 2 Cloud and Aerosol Profile Products Version Releases: 3.01, 3.02.

NASA CALIPSO team (2012b), CALIPSO Quality Statements Lidar Level 2 Cloud and Aerosol Layer Products Version Releases: 3.01, 3.02.

National Centers for Environmental Prediction/National Weather Service/NOAA/U.S. Department of Commerce (2000), NCEP FNL Operational Model Global Tropospheric Analyses, continuing from July 1999. doi: 10.5065/D6M043C6, Research Data Archive at the National Center for Atmospheric Research, Computational and Information Systems Laboratory.

Platnick, S., M. D. King, and K. G. Meyer (2015a), MODIS cloud optical properties: user guide for the collection 6 level-2 MOD06/MYD06 product and associated level-3 datasets.

Platnick, S., S. Ackerman, M. King, G. Wind, K. Meyer, P. Menzel, R. Frey, R. Holz, B. Baum, and P. Yang (2015b), MODIS atmosphere L2 cloud product (06_L2). doi: 10.5067/MODIS/MYD06_L2.006, NASA MODIS Adaptive Processing System, Goddard Space Flight Center.

PSU (2017), STAT 505 - Applied Multivariate Statistical Analysis, available at https://onlinecourses.science.psu.edu/stat505/node/.

Remer, L. A., et al. (2005), The MODIS aerosol algorithm, products, and validation, *J Atmos Sci*, *62*(4), 947-973.

Zhao, B., et al. (2018), Impact of aerosols on ice crystal size, *Atmos Chem Phys*, *18*, 1065-1078.